Revealing Order and Disorder in Films and Single Crystals of a Thiophene-Based Oligomer by Optical Spectroscopy

Sajedeh Motamen[1], Dominic Raithel[2], Richard Hildner[2], Khosrow Rahimi[3], Thibaut Jarrosson[4], Françoise Serein-Spirau[4], Laurent Simon[5], Günter Reiter[1]

[1]Physikalisches Institut, Albert-Ludwigs-Universität, 79104 Freiburg, Germany

[2] Experimentalphysik IV, University of Bayreuth, 95440 Bayreuth, Germany

[3] DWI-Leibniz Institute for Interactive Materials, Forckenbeckstr. 50, 52056 Aachen, Germany

[4] Institut Charles Gerhardt de Montpellier, UMR 5353-CNRS Equipe Architectures Moleculaires et Matériaux Nanostructurés (AM2N), Ecole Nationale Supérieure de Chimie de Montpellier, 8 Rue de l'Ecole Normale, 34296 Montpellier cedex 05, France

[5] Institut de Sciences des Matériaux de Mulhouse IS2M, UMR7361 CNRS-UHA, 3 bis rue Alfred Werner, 68093 Mulhouse, France.
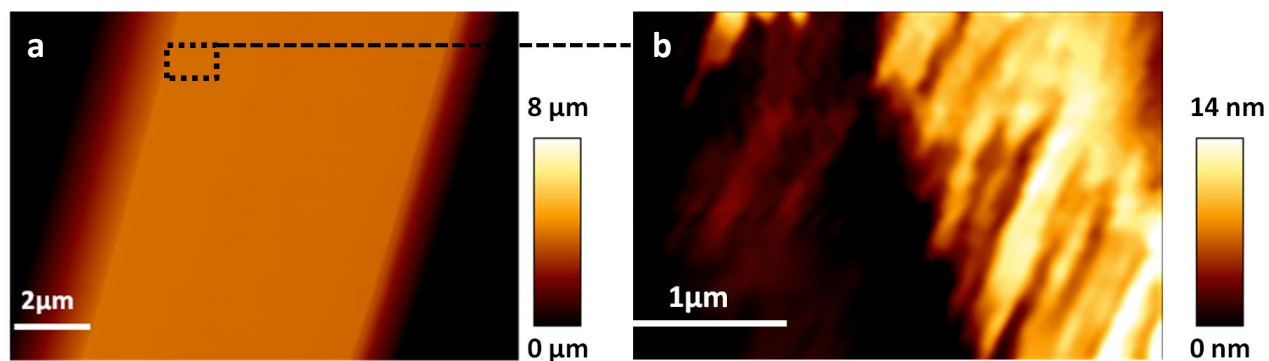
AFM Measurements:

Figure S1: a) AFM height image of a 3TBT single crystal obtained by crystallization at 60 °C from a 0.1 g/L solution in dodecane and spin-coated onto a solid substrate. b) AFM height image of the area within the dashed box in a) showing fluctuations of height on the surface of the crystal.
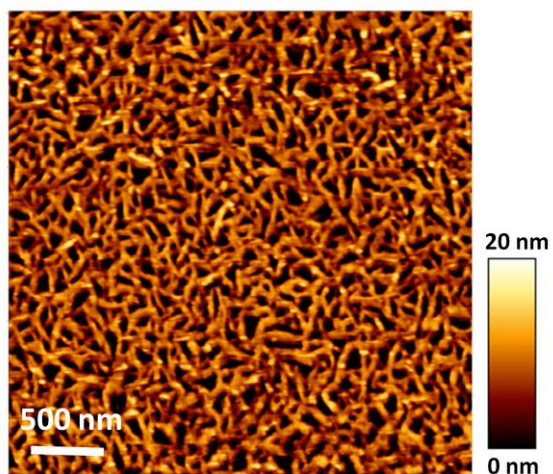

Figure S2: AFM height image of a 3TBT thin film (15±3 nm) spin coated from solution onto a solid substrate (2 g/L in dodecane).

Absorbance Measurements:

   In order to determine the electronic interaction between nearest-neighbor 3TBT molecules in single crystals and in nanoscale aggregates in spin-coated films, we analyzed the corresponding room temperature absorption spectra. The absorption from both samples exhibits a pronounced peak around 2.7 – 2.8 eV (see Figure 2a and S3), which indicates the presence of a non-negligible fraction of non-aggregated ("amorphous") 3TBT molecules. To correct the measured film and crystal spectra for the absorption of non-aggregated molecules, we scaled and shifted the solution absorption (Figure. 2a, red spectrum), such that we obtain the best fit to the highest-energy part of both the film and crystal absorption. The best agreement is achieved with a blue shifted solution spectrum by 120 meV (see Figure S3); this spectral shift represents a polarization energy and accounts for different dielectric environments for the non-aggregated 3TBT molecules (solution: solvent; film/crystal: 3TBT). Note that especially the film spectrum is not perfectly reproduced at high energies, which may be due to scattering on the nanoscale crystallites (see Figure S2). Subsequently, we subtracted the scaled and shifted "solution" spectrum to obtain the absorption spectrum exclusively of interacting 3TBT molecules in crystals/films.

   This latter spectrum is then numerically simulated based on the framework developed by Spano and co-workers[1,2], which allows to retrieve the nearest-neighbor electronic interaction between 3TBT molecules.

   These simulations required as input parameters the Huang-Rhys factor S and the vibrational energy E_{vib} of the dominating aromatic carbon-bond stretch mode of isolated, non-interacting 3TBT molecules, which we determined from the PL spectrum of molecularly dissolved 3TBT in dodecane (see Figure. 2b of the main text) to $S = 0.85$ and $E_{vib} = 170$ meV. Moreover, we limited the number of interacting 3TBT molecules to 20, which is a compromise between size of the system and computational time. The best agreement between experiment and simulations was obtained using a free exciton bandwidth W of 164 meV for the crystal and 43 meV for the film (Figure S3). Because W is related to the nearest-neighbor interaction J by $W = 4J$, we finally get $J = 41$ meV (crystal) and $J = 11$ meV (film).
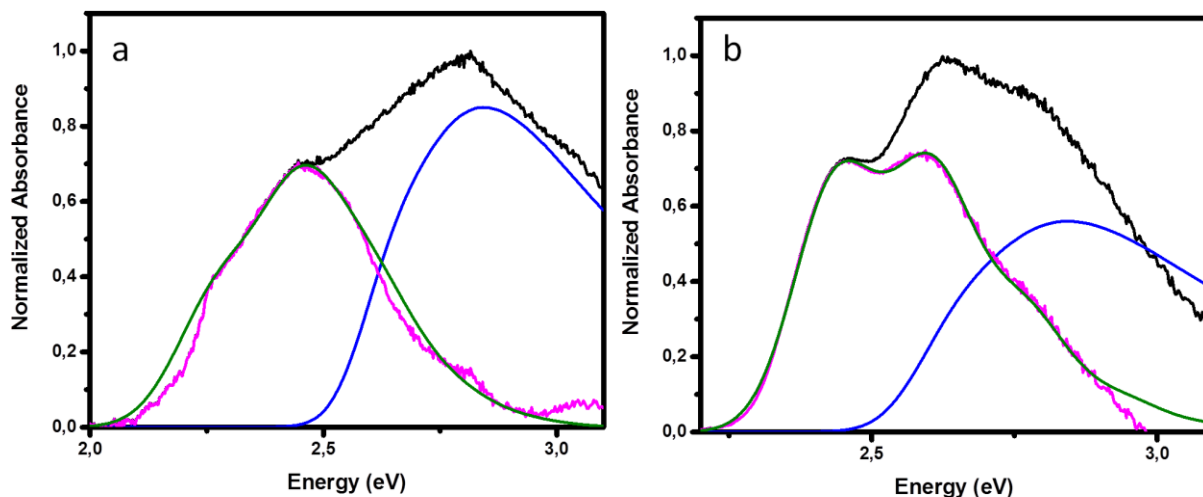
Figure S3: a) Normalized absorbance spectrum of a 3TBT single crystal (black), the scaled and spectrally shifted solution absorption (blue), the difference spectrum (pink), and the simulated spectra (green). (b) Normalized absorbance spectrum of a spin-coated 3TBT film (black), the scaled and spectrally shifted solution absorption (blue), the difference spectrum (pink), and the simulated spectra (green).

In principle, the data in Figure S3 allow to retrieve the fraction of non-interacting 3TBT molecules in both samples from the relative areas under the scaled and shifted solution absorption and the difference spectrum (weighted by the different oscillator strengths for aggregates and non-interacting molecules). For the spectrum of the spin-coated film the relative areas are 45 % for the solution contribution and 55 % for the remaining aggregate spectrum. Hence, there is still a substantial fraction of non-interacting molecules, which is expected as a result of very fast evaporation of the solvent. For the measured crystal spectrum, we obtain a similar ratio of areas: 55 % for solution and 45 % for the crystal contribution. This large fraction of non-interacting molecules in the crystal spectrum is clearly a strong overestimation, because in the measured crystal spectrum also the absorption of a fraction of nanoscale aggregates (as in spin-coated films) will contribute (see AFM image in Figure S1b). We note that a deconvolution of the total crystal absorption spectrum into "true" crystal, nanoscale aggregate and solution contribution to obtain the relative areas, was not possible (in fact such deconvolution would require prior knowledge of the relative areas and exact

polarization energies of all contributions, which is not available). From the AFM data (Figure S1), we can estimate a non-crystalline contribution of about 10 %. Also from the sharply peaked dichroic ratio of the crystal (Figure 3b) the contribution of both the nanoscale aggregate and solution contribution to the measured crystal absorption is visible. The nanoscale aggregates absorb at 2.4 eV and higher energies (Figure S3b), yet their orientations on the crystal are not unique as for the crystal orientation itself (see Figure S1b), and hence, absorption of the aggregates will not show a strong polarization dependence. This explains why the dichroic ratio is strongly peaked only around 2.25 eV, where exclusively the crystal with its strongly polarization-dependent absorption contributes.

PL Measurements:

The room-temperature PL spectra of a 3TBT film and a single crystal exhibit three peaks/shoulders with an energy spacing of approximately 170 meV (1400 cm^{-1}), representing the purely electronic transition, a vibronic transition into the aromatic carbon-bond stretch and its overtones (0-0, 0-1, 0-n) (Figure S4 and S5). However, fitting of these spectra with three Gaussian functions was not possible, only a fit with five Gaussians yielded satisfactory results. The full width at half maximum (fwhm) and the area of the Gaussians were treated as adjustable parameters to give the best fit to the experimental data. We attempted to represent the data by the smallest as possible number of different vibronic families. In the fits in Figure S4 and S5 the red curves represent the carbon-carbon bond stretch vibration with energy of 170 meV (1400 cm^{-1}), while the blue and pink curves can be attributed to (superpositions of) other intra-molecular vibrations of 3TBT based on low-temperature spectra (see Figure S7).
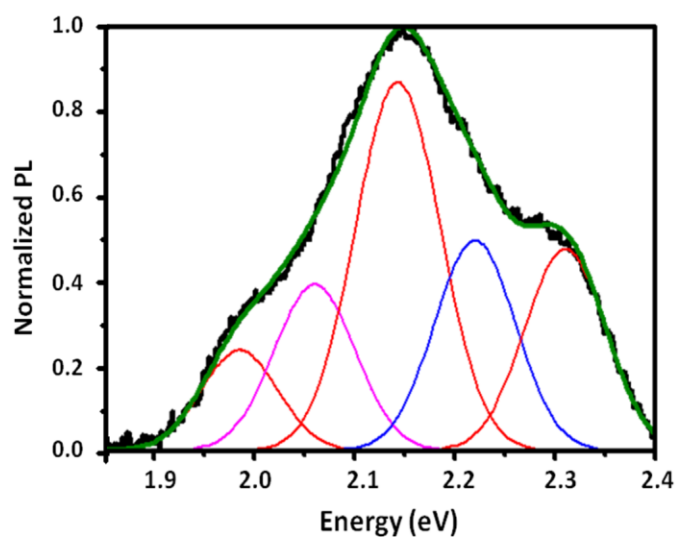
Figure S4: Normalized PL spectrum (black curve) of 3TBT **film** at room temperature, together with a fit (green curve) of five Gaussian peaks.

Gaussian	Peak Position [eV]	Integrated Area	Full Width at Half Maximum FWHM [eV]	Intensity at Peak Position [Counts]	Relative Integrated Area [%]
Peak 1	2.31	0.047	0.095	0.475	18.89
Peak 2	2.22	0.050	0.095	0.496	19.84
Peak 3	2.143	0.092	0.1	0.869	36.62
Peak 4	2.06	0.039	0.095	0.391	15.67
Peak 5	1.985	0.022	0.09	0.236	8.95

TableS1. Fitting parameters used for the decomposition of photoluminescence spectra of the film.
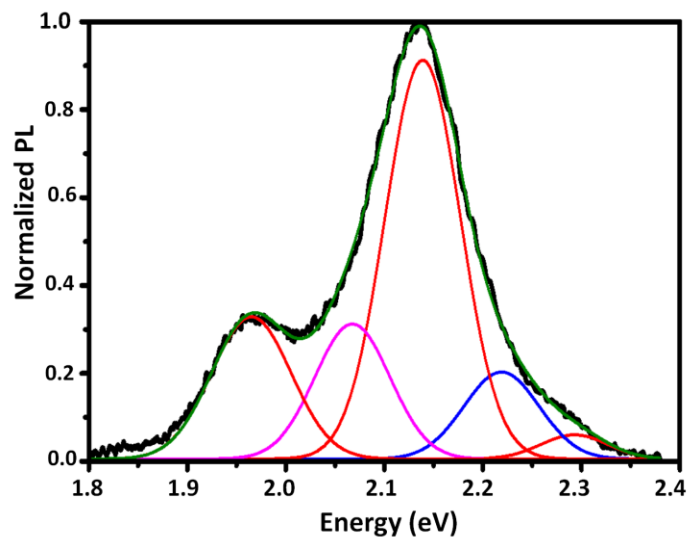
Figure S5: Normalized PL spectrum (black curve) of a 3TBT **crystal** at room temperature, together with a fit (green curve) of five Gaussian peaks to reproduce the vibronic structure. The diameter of the detection area was 1 µm and the width of crystal was 4 µm.

Gaussian	Peak position [eV]	Integrated Area	Full Width at Half Maximum FWHM [eV]	Intensity at Peak Position [Counts]	Relative Integrated Area [%]
Peak 1	2.293	0.004	0.08	0.05	2.70
Peak 2	2.22	0.019	0.09	0.20	10.97
Peak 3	2.14	0.087	0.09	0.90	50.33
Peak 4	2.064	0.029	0.09	0.30	17.03
Peak 5	1.965	0.033	0.095	0.32	18.95

TableS2. Fitting parameters used for the decomposition of photoluminescence spectra of the crystal.
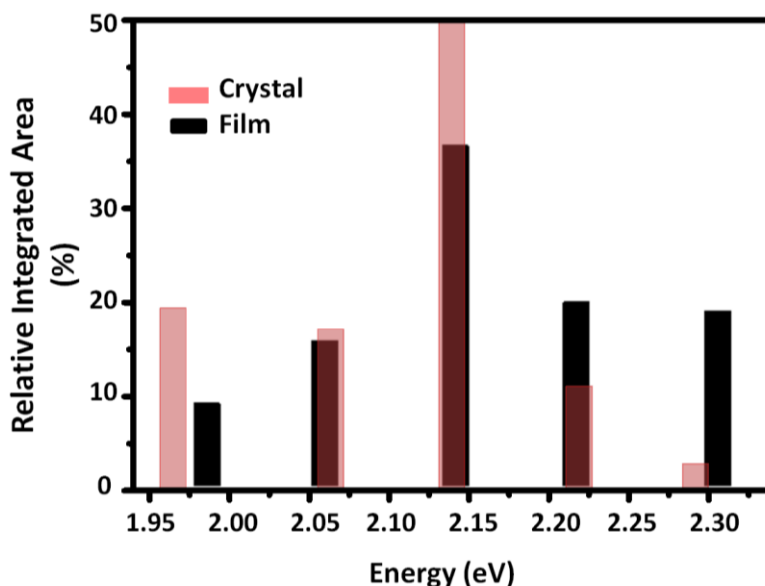
Figure S6: Relative integrated area of five Gaussian peaks fit to the PL spectra of a 3TBT crystal and film at room temperature a function of emitting energy. Width of errors was chosen 0.02 eV.

Low temperature measurements were done using a home-built confocal microscope with a spot size of ~ 600 nm diameter and a pulsed 450 nm diode–laser for excitation. The sample was placed inside of a helium bath-cryostat and cooled to 1.5 K. Low temperature PL spectra from a single crystal exhibited three dominating peaks and a rich sub-structure with minor peaks and shoulders (Figure S7 and table S3). Hence, a decomposition required eight Gaussian peaks. Peak A can be ascribed to the purely electronic 0-0 transition of the PL of the 3TBT crystal. The peaks B – H are attributed to intra-molecular vibrations coupling to the electronic transition based on literature data[3–5]: Peak B (29 meV or 232 cm^{-1} relative to the 0-0 transition) is attributed to a superposition of a stretching vibration of the 3TBT backbone, a libration motion of the rings within the 3TBT backbone, and in- and out-of-plane bending. Peaks C (84 meV, 670 cm^{-1}) and D (122 meV, 976 cm^{-1}) stem from ring breathing/deformation modes of thiophene and benzene as well as from CCH-bending and COC- and CS-stretch modes. In most thiophene-based molecules, the aromatic carbon bond stretch with energies around 170 meV (1400 cm^{-1}) couple strongly to the electronic transition, which corresponds to peak E. Consequently, peak H (364

meV, 2910 cm^{-1}) represents the overtone of the aromatic carbon-bond stretch mode E. Peak F (229 meV, 1832 cm^{-1}) may be caused by a carbon-carbon double-bond stretching mode. Peak G (295 meV, 2360 cm^{-1}) is probably a combination vibration, e.g. from peak D and peak E. From this assignment it is clear that most of the eight peaks that are resolved in the low temperature PL spectrum are in fact a superposition of several unresolvable vibrational modes, i.e. vibrational modes with energy separations smaller than the inhomogeneous width. Hence, the use of different line widths for the different peaks is justified. We note that a fit using the same width for all vibronic lines requires in total 10 to 12 Gaussian functions to reproduce the low temperature PL spectrum with the same quality and over the same spectral range. Yet, in this spectrum we can not identify that many peaks and shoulders, and we therefore did limit ourselves to 8 Gaussians only.

The appearance of this rich vibrational structure in the 1.5 K PL spectrum compared to the room temperature PL can be traced back to the strong reduction of the homogeneous line width upon cooling down. Typically, for large organic molecules, such as conjugated polymers and oligomers, the homogeneous line width is below 0.13 meV (1 cm^{-1}) at 1.5 K[6–8]. Hence, line broadening is dominated by inhomogeneous broadening and all (groups of) vibrational modes with energy separations larger than the inhomogeneous width can be discriminated as distinct peaks/shoulders in the low temperature PL. From the width of the 0-0 transition (peak A, Figure S7 and table S3) the inhomogeneous line width at 1.5 K can be estimated to about 33 meV. In contrast, at room temperature the homogeneous line width is up to 60 meV (~ 500 cm^{-1}). Consequently, neighboring lines separated by less than ca. 60 meV cannot be resolved as distinct lines any more (neglecting a possible increase in the inhomogeneous line width with increasing temperature due to increasing thermal disorder). This means that peaks A and B of the low temperature spectrum with an energy separation of only 29 meV appear as a single broad line (peak 1) in the room temperature PL; similarly peaks C and D merge into peak 2; finally, peaks F and G give peak 4. Only the strong aromatic carbon-bond stretch (peaks E and H at 1.5 K) still appears as clearly distinct peaks at room temperature as well (peaks 3 and 5).
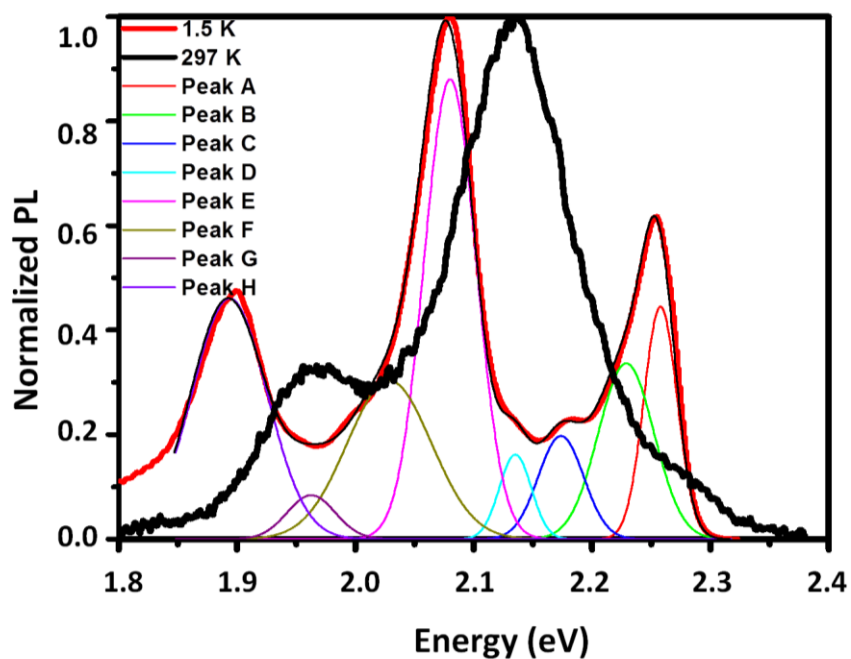
Figure S7: Normalized PL spectra of 3TBT crystal at 1.5 K (red curve) and at room temperature (black curve) were fit to families of Gaussian functions to reproduce the vibronic structure.

Gaussian	Peak Position [ev]	Full Width at Half Maximum FWHM [eV]	Integrated Area
Peak A	2.257	0.033	10.19
Peak B	2.228	0.055	11.33
Peak C	2.173	0.045	4.71
Peak D	2.135	0.0318	2.52
Peak E	2.080	0.051	32.19
Peak F	2.028	0.083	15.73
Peak G	1.962	0.048	1.22
Peak H	1.893	0.075	22.07

TableS3. Fitting parameters used for the decomposition of photoluminescence spectra of the single crystal at 1.5K.

Finally, we note that the relative 0-0 peak intensity decreases from 1.5 K to room temperature and thus shows an unusual temperature-dependence. This behavior cannot be explained in a straightforward way with Spano's approach, because upon heating up the thermal disorder in the crystal increases which is expected to increase the relative 0-0 peak intensity[9,10]. However, in an perturbative ansatz Spano showed that the 0-0/0-1 intensity ratio is inversely proportional to the square of the free exciton bandwidth W in a regime where energy disorder is not too large[9,10]. If we then assume that at 1.5 K the 3TBT molecules in the crystal are nearly perfectly arranged and planar, i.e. electronic excitations are fully delocalized over a molecule, whereas at higher temperatures thermal energy allows for small torsional degrees of freedom of 3TBT, which slightly localizes electronic excitations. Owing to this reduction in delocalization, the nearest-neighbor interaction between 3TBT molecules increases with increasing temperature, and thus the 0-0/0-1 intensity ratio decreases (again: if disorder does not increase too strongly). Since it is very difficult, however, to unambiguously determine the energy disorder from our data, we do not wish to make any quantitative statements as to the temperature-dependence of the 0-0/0-1 intensity ratio. The 1.5 K PL spectrum is only meant to justify the use of 5 Gaussian peaks for the fitting of the room temperature data.

Moreover, there are some limitations of Spano's theory: only a single effective vibrational mode is included, whereas we clearly do see a rich vibronic structure; especially low energy vibrational modes exhibit a strong temperature dependence, which is also not included in this theoretical framework; only nearest-neighbor interactions are considered, which is a rather strong approximation for a densely packed system as represented by a 3TBT crystal. Probably, a combined quantum chemistry/molecular mechanics approach as used by Beljonne, Gierschner et al. might be more suited to reproduce the temperature-dependence of our PL spectra[11].

An alternative interpretation for this unusual temperature-dependence of the relative 0-0 peak intensity are temperature-dependent energy transfer rates between disordered and ordered regions of the samples. In our PL experiments we predominantly excite disordered regions (excitation energy ~ 2.66 eV, compare Figures 2a, 3b, and S3), from where ordered regions are populated by incoherent hopping processes prior to emission. The transfer rate for incoherent hopping, however, increases with increasing temperature[12], i.e. this transfer is slower at 1.5 K

than at room temperature. Consequently, at low temperatures we may expect emission also from more disordered regions due to incomplete energy transfer to ordered regions. This results in PL spectra with a larger relative 0-0 peak intensity. In contrast, at room temperature this energy transfer is fast and thus highly efficient, which results in emission from nearly exclusively highly ordered regions with a small relative 0-0 peak intensity. Since we cannot deduce the energy transfer rates from our PL measurements, we unfortunately cannot tell which mechanism is responsible for the unusual temperature-dependence of the relative 0-0 peak intensity.
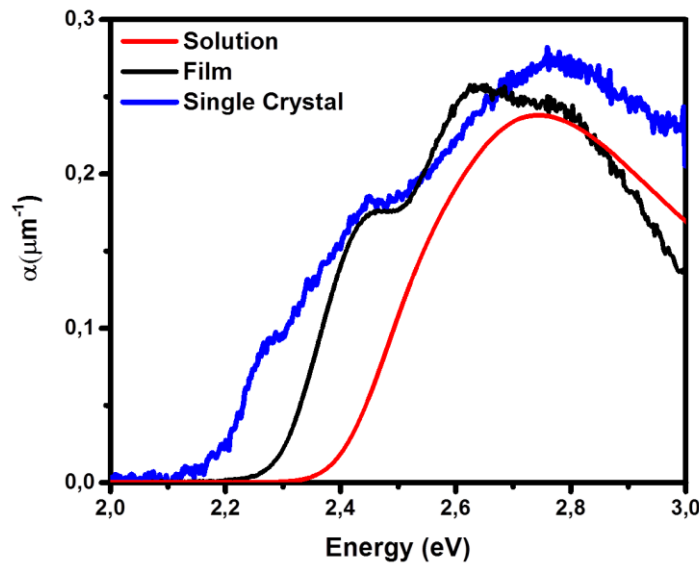

Figure S8: Absorption coefficient of solution (red), film (black) and crystal (blue).

Optical Density of Solution, Film and Single Crystal:

We calculated the absorption coefficient (α) for the film and the single crystal according to the Beer–Lambert law: $A = -\log T = -\frac{1}{\ln 10} \ln T$ with A being the absorbance. The transmittance (T) is defined by: $T = \exp(-\alpha z)$.

Then $A = \frac{\alpha z}{\ln 10} \approx 0.4343 \alpha z$, where z is the thickness of the crystal. The extinction coefficient (ϵ) for the solution was calculated by using: $A = \epsilon c l$, where c is the concentration of the solution and l is the length of the optical path (thickness of the solution).

Figure S8 shows the absorption coefficient of the solution (measuring the absorption of light for an optical path of 1µm in the solution), film and crystal. All values are of the same order of magnitude, consistent with results obtained for P3HT by Clark et al[13].

Comparison of PL spectra of Crystal Measured at Different Polarization Direction:

In Figure S9a, we scaled up the emission spectrum at $\psi = 0°$ (i.e., emitted light is polarized in the direction of the long axis of the crystal). As seen in Figure S9, the intensity ratio I_{0-1}/I_{0-0} decreased by changing the angle between the long axis of the crystal and the analyzer from 90° to 0°. This is related to the different absorptions for light polarized perpendicular ($\psi = 90°$) and parallel ($\psi = 0°$) to the long axis of the crystal. For PL in the energy range 2.3 eV with polarization parallel ($\psi = 0°$) to the long axis the overlap with the absorption is negligible, as evident from the corresponding absorption spectrum (Figure 3a, red line). Hence, reabsorption does not take place. For light polarized perpendicularly, there is some overlap between absorption and emission, and some reabsorption takes place. These data provide further evidence that reabsorption is only a minor effect in our PL spectra of crystals, and cannot account for the difference between film and crystal PL.

Figure S9b, shows normalized PL spectra taken at the center and the edge of the crystal. By moving the detection area (diameter of 4 µm) from the ordered (crystalline) to the disordered (film) region, the intensity ratio I_{0-1}/I_{0-0} changed from 17 to 5. When changing the angle between the long axis of the crystal and the analyzer from 90° to 0°, the intensity ratio I_{0-1}/I_{0-0} decreased from 12 to 6.5 (Figure S9a). In other words, although reabsorption probably contributes in the change of this I_{0-1}/I_{0-0} ratio, reabsorption certainly cannot account for observed change in this ratio when going from the centre to the edge of the crystal.

Furthermore, we have measured dichroic ratio at the center, edge and far outside of the crystal. Figure S9c clearly shows that the dichroic ratio decreased by moving the detection area from the ordered (crystalline) to the disordered (film) region. These results confirm that changing the contribution of ordered region in the detection area influences the emission spectra with respect to the dichroic ration and the intensity ratio I_{0-1}/I_{0-0}.
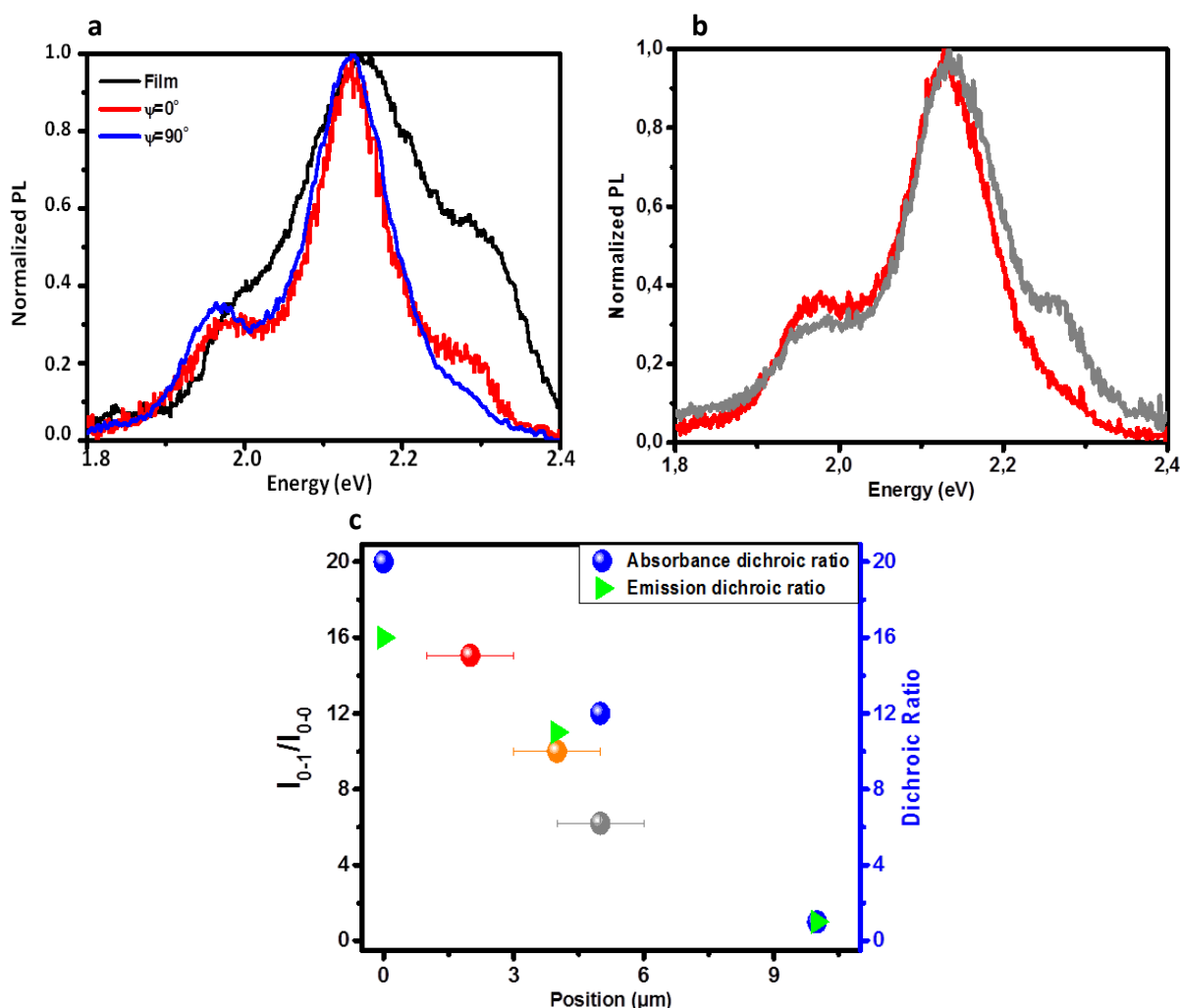
Figure S9: a) Normalized PL spectra of a 3TBT single crystal measured at the center of the crystal at normal incidence (dichroic ratio is 15), where ψ is the angle between the long axis of the crystal and analyzer together with the normalized PL spectrum from an as-cast 3TBT film. b) Normalized PL spectra taken at the edge (gray) and center of the crystal (red). c) Intensity ratio I_{0-1}/I_{0-0} as a function of the distance to the center of the crystal, compared with the corresponding dichroic ratio (blue and green).

References:

(1)   Spano, F. C. The Spectral Signatures of Frenkel Polarons in H- And J-Aggregates. *Acc. Chem. Res.* **2010**, *43*, 429–439.

(2)   Spano, F. C. Modeling Disorder in Polymer Aggregates: The Optical Spectroscopy of Regioregular poly(3-Hexylthiophene) Thin Films. *J. Chem. Phys.* **2005**, *122*.

(3)   Degli Esposti, a; Moze, O.; Taliani, C.; Tomkinson, J. T.; Zamboni, R.; Zerbetto, F. The Intramolecular Vibrations of Prototypical Polythiophenes. *J. Chem. Phys.* **1996**, *104*, 9704–9716.

(4)   Bouachrine, M.; Bouzakraoui, S.; Hamidi, M.; Ayachi, S.; Alimi, K.; Lère-Porte, J. P.; Moreau, J. Synthesis and Characterization of Co-Polymers Involving Various Thiophene and Phenylene Monomers. *Synth. Met.* **2004**, *145*, 237–243.

(5)   Hermet, P.; Lois-Sierra, S.; Bantignies, J. L.; Rols, S.; Sauvajol, J. L.; Serein-Spirau, F.; L??re-Porte, J. P.; Moreau, J. J. E. Lattice Dynamics of Oligo(phenylenethienylene)s: A Far-Infrared and Inelastic Neutron Scattering Study. *J. Phys. Chem. B* **2009**, *113*, 4197–4202.

(6)   Baderschneider, S.; Scherf, U.; Köhler, J.; Hildner, R. Influence of the Conjugation Length on the Optical Spectra of Single Ladder-Type (p-Phenylene) Dimers and Polymers. *J. Phys. Chem. A* **2016**, *120*, 233–240.

(7)   Lang, E.; Hildner, R.; Engelke, H.; Osswald, P.; Würthner, F.; Köhler, J. Comparison of the Photophysical Parameters for Three Perylene Bisimide Derivatives by Single-Molecule Spectroscopy. *ChemPhysChem* **2007**, *8*, 1487–1496.

(8)   Feist, F. a.; Tommaseo, G.; Basché, T. Observation of Very Narrow Linewidths in the Fluorescence Excitation Spectra of Single Conjugated Polymer Chains at 1.2 K. *Phys. Rev. Lett.* **2007**, *98*, 1–4.

(9)   Spano, F. C.; Clark, J.; Silva, C.; Friend, R. H. Determining Exciton Coherence from the Photoluminescence Spectral Line Shape in poly(3-Hexylthiophene) Thin Films. *J. Chem. Phys.* **2009**, *130*, 1–16.

(10)   Spano, F. C. Modeling Disorder in Polymer Aggregates: The Optical Spectroscopy of Regioregular poly(3-Hexylthiophene) Thin Films. *J. Chem. Phys.* **2005**, *122*.

(11)   Wykes, M.; Parambil, R.; Beljonne, D.; Gierschner, J. Vibronic Coupling in Molecular Crystals: A Franck-Condon Herzberg-Teller Model of H-Aggregate Fluorescence Based on Quantum Chemical Cluster Calculations. *J. Chem. Phys.* **2015**, *143*.

(12)   Scholes, G. D. L Scholes, G. D. L Long-Range Resonance Energy Transfer in Molecular Systems. *Annu. Rev. Phys. Chem.* **2003**, *54* (1), 57–87.

(13)   Clark, J.; Chang, J. F.; Spano, F. C.; Friend, R. H.; Silva, C. Determining Exciton Bandwidth and Film Microstructure in Polythiophene Films Using Linear Absorption Spectroscopy. *Appl. Phys. Lett.* **2009**, *94*, 2007–2010.